

## Modeling the Mass Distribution of Binary Black Hole Mergers with GWTC-3 LIGO Surf 2022 Interim Report 1

JINGYI ZHANG,<sup>1</sup> SUPERVISED BY: ALAN J. WEINSTEIN,<sup>2</sup> AND JACOB, GOLOMB<sup>2</sup>

<sup>1</sup>*Smith College*

<sup>2</sup>*LIGO Laboratory, California Institute of Technology*

### 1. MOTIVATION: BLACK HOLE POPULATION IN THE UNIVERSE

With roughly 70 binary black hole merger (BBHs) events detected by the Advanced LIGO and Advanced Virgo Scientific Collaboration, it is possible to infer the overall character of black hole population in the universe. Based on the third Gravitational-wave Transient Catalog (GWTC-3), [The LIGO Scientific Collaboration et al. \(2021\)](#) looked into the mass and spin distribution, overall merger rate, as well as the cosmological evolution of binary black holes. These information provides valuable information on high mass star formation and history of stellar evolution, as well as how compact objects fit in the evolution of the universe.

The BBHs population has been fitted with models and described with the associated population hyper-parameters. For example, Figure 1 shows the estimated primary mass distribution of BBHs using the currently most commonly accepted *POWER LAW + PEAK* model (PP) model.

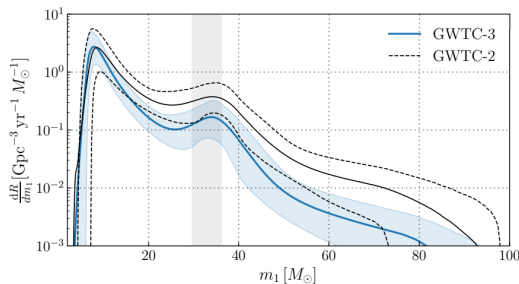


**Figure 1.** Probability density function of the primary mass distribution for the fiducial Power-Peak (PP) model. (For more on the model, please see [Talbot & Thrane \(2018\)](#)) The solid lines show the posterior population distribution (PPD) and the region shows the 90 percent credible interval of GWTC-3 (blue) and GWTC-2 (black), respectively. As shown in the figure, GWTC-3 suggests that the primary mass has more prominent peaks than we previously observed. ([The LIGO Scientific Collaboration et al. 2021](#))

Aiming to evaluate the parameter estimation’s performance, compare different black hole population models, discuss effects of outliers, and improve the general modeling process; we want to conduct goodness-of-fit tests on each step of the hyper-parameter estimation. In addition to supplement the GWTC-3 estimations, the test can also help to better understand the expected population from the upcoming forth observation run (O4.) For this project, I focus on the mass distribution of BBHs.

### 2. METHODS: STRAIN, EVENTS, AND POPULATION

We obtained the estimation of hyper-parameters with two steps. First, mass, spin, redshift, inclination, etc. of the individual BBHs are estimated from the strain data from the interferometer. The individual BBHs parameters are then used to estimate the astrophysical distribution of the population. The two-step approach, also known as the hierarchical Bayesian inference ([Talbot et al. 2019](#)), is described below.

#### 2.1. Single event parameters

15 parameters describes an individual BBHs events: 8 intrinsic parameters that characterized the spin and mass of the two black holes, 7 extrinsic parameters that describe the binary’s position and orbit as seen by us. Packages such as BILBY ([Ashton et al. 2019](#)) and LAL-INFERENCE ([Veitch et al. 2015](#)) use bayesian inference to estimate the parameters from the strain data. (Figure 2.) The result is given in the form of posterior samples. Each sample contain a possible combination of the parameters that may create the observed signal. The distribution of parameters in the posterior sample represent the probability distribution of each parameters including how they may be correlated, as shown in Figure 3. One thing to note is that the estimated parameters are in the detector frame, the properties we see on earth. However, many BBHs events happened far away enough that we must take cosmology into consideration. We can directly estimate the luminosity distance from the strain data. With the assumption of current date cosmological

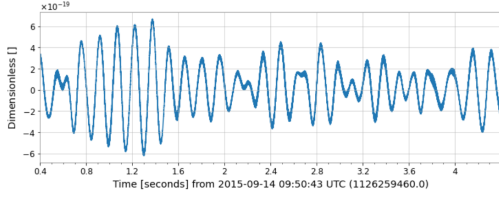


**Figure 2.** The strain data of BBHs event GW150914 at the LIGO Hanford observatory. The strain contains 4 seconds of data around the event. (Abbott et al. 2021)

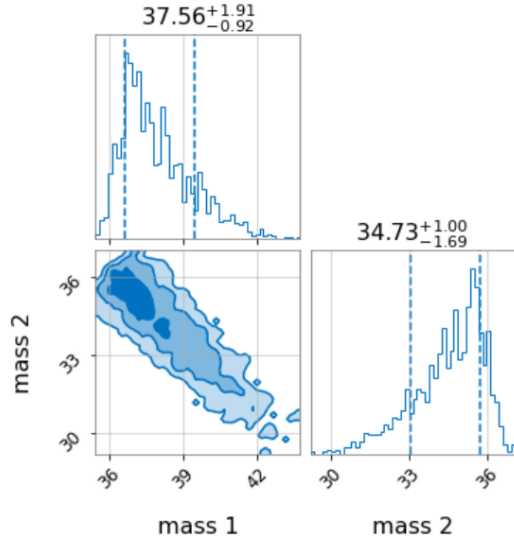


**Figure 3.** The posterior distribution of primary mass ( $m_1$ ), and secondary mass ( $m_2$ ) of GW150914 and their correlation. In this corner plot, all other parameters are marginalized. The dotted line marked the 90 percent credibility interval—90 percent of the posterior sample is in this mass range.

parameters, we can calculate the redshift of the event. (Hogg 1999) The redshift can then be used to calculate the source frame parameters of the events. The source frame parameter is independent of the observer and reflect the astrophysical information that we would like to use.

## 2.2. Population Hyper-Parameters

Similar to single event parameter estimation where we take in observed strain data as the likelihood to obtain the posterior distribution, (In this case, as we don't know much about the event, we use uninformative prior in the bayesian inference.) we use "data" of the individual events to obtain posterior distribution of the population hyper-parameter. Here, the "data" is the parameter estimation of all events.

We first define the hyper-parameters we want to estimate with our model. For instance, the most important ones of the *POWER LAW + PEAK* model are the index

of the power law, the lower mass cutoff, the position of the peak, the width of the peak, and the contribution of the peak in the entire distribution. Several other hyper-parameters describe the detailed shape of the distribution, but they may not be as important.

With the hyper-parameters defined, we can construct the likelihood for the bayesian inference. For each BBHs, we can calculate the probability of getting such events under a defined population model (the model is characterized with hyper-parameters). Given that all events are independent, the probability of getting all the events—the likelihood—is the product of all individual probability.

$$\mathcal{L}(d|\Lambda) = \prod_i^N P(\theta_i|\Lambda) \quad (1)$$

Where  $\Lambda$  is the hyper-parameter and  $\theta_i$  is the parameter of the  $i^{th}$  event.

However, we do not have the exact value of the parameter describing each single events. We can only infer their probability distribution from the strain data.

$$\mathcal{L}(d|\Lambda) = \prod_i^N \int d\theta_i \mathcal{L}(d_i|\theta_i) p(\theta_i|\Lambda) \quad (2)$$

Here the  $\mathcal{L}(d_i|\theta_i)$  term is the probability of getting  $\theta_i$  for the  $i^{th}$  event given the strain data. We integrate over all  $\theta_i$  that we can get from the strain data to get the total probability, hence the  $\int d\theta_i \mathcal{L}(d_i|\theta_i)$  term. In reality, we do not have a smooth probability distribution, but rather discrete samples that represent the events. The number of samples represent the probability (similar to how histogram is used to describe probability density.) Instead of reintegration, we add up the probability of each sample to construct our hyper-parameter likelihood.

$$\mathcal{L}(d|\Lambda) = \prod_i^N \sum_{\theta_i \sim \mathcal{L}(d_i|\theta_i)} p(\theta_i|\Lambda) \quad (3)$$

Finally, like all other astronomical observation, gravitational detection is subjected to selection effect: more massive black holes that create stronger signals are easier to detect. We correct this bias by including a "detection probability" term.

$$\mathcal{L}(d|\Lambda) \propto \frac{\prod_i^N \int d\theta_i \mathcal{L}(d_i|\theta_i) p(\theta_i|\Lambda)}{p_{\text{det}}(\Lambda)^N} \quad (4)$$

$$p_{\text{det}}(\Lambda) = \int p(\theta|\Lambda) p_{\text{det}}(\theta) d\theta \quad (5)$$

The "detection probability" term include the probability of detecting each parameter and the probability of detection such parameter under certain model.

124 With the likelihood defined, we pass it to python pack-  
 125 age GWPOPULATION to define do the bayesian inference.

126 3. PROJECT: GOODNESS-OF-FIT

127 For my specific project, we want to conduct multi-  
 128 ple goodness-of-fit test to test the accountability of the  
 129 analysis process as well as better understand the effect  
 130 of data and models in the analysis.

131 1. Single and Multiple Parameter Goodness-of-Fit  
 132 Test We want to test how well the GWTC-3 (The  
 133 LIGO Scientific Collaboration et al. 2021) popu-  
 134 lation estimation agrees with the predicted distri-  
 135 bution. We may use the model to generate events  
 136 arbitrarily, and see how well we can recover the  
 137 model through the analysis process, similar to the  
 138 comparision we conduct between the GWTC-2 and  
 139 GWTC-3 estimation in Figure 4. (The LIGO Sci-  
 140 entific Collaboration et al. 2021) We may conduct  
 141  $\chi^2$  test or Kolmogorov–Smirnov test (ks-test) to  
 142 compare the resulting posterior distribution with  
 143 the model.

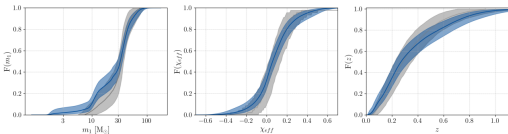


**Figure 4.** The empirical cumulative density function of primary mass, effective inspiral spin, and redshift. The blue region represent the distribution from GWTC-3, while the grey represent the distribution from GWTC-2. The solid lines show the median while the shaded area are 90 percent credible interval. (The LIGO Scientific Collaboration et al. 2021) For this project, we hope to conduct similar comparison between the observed GWTC-3 population and the theoretical modeled population.

144 2. Leave-One-Out Test In the analysis of the GWTC-  
 145 3 population, outliers with extreme mass values

146 were left out because they significantly changed  
 147 the posterior result and does not agree with the  
 148 prediction generated by the others. This leave us  
 149 to wonder whether other events that are included  
 150 in the analysis would also significantly change  
 151 the result, and what are the impact of individ-  
 152 ual events. We may test this by run the estima-  
 153 tion many times with one events excluded for each  
 154 run. Noted that though some events are marked  
 155 as “outliers”, they still bear astrophysical signifi-  
 156 cance.

157 3. Model Comparison The currently most commonly  
 158 used *POWER LAW + PEAK* (Talbot & Thrane  
 159 2018) model consist of two parts: a power law moti-  
 160 vated by the initial mass function (IMF) of stel-  
 161 lar formation, where higher mass stars are much  
 162 rarer than the low mass ones, and a peak moti-  
 163 vated by the pulsational pair-instability super-  
 164 novae (PPSN) graveyard, where stars over a cer-  
 165 tain threshold would experience explosions and  
 166 leave remnants of similar masses after the super-  
 167 novae. However, this is not the only model that  
 168 describe the binary black hole population. Other  
 169 parametric model describe the lower and higher  
 170 mass cutoff differently, and hierarchical mergers  
 171 may create additional peaks in the mass distribu-  
 172 tion. Other models attempt to describe the dis-  
 173 tribution with non-parametric models, where the  
 174 distribution is almost solely rely on the observed  
 175 data. We want to see how the posterior distribu-  
 176 tion change when assuming different models. By  
 177 comparing the Bayes factor, We want to inves-  
 178 tigate that whether other models can also yield  
 179 nicely-fitted result and whether we should consider  
 180 them for later analysis.

REFERENCES

181 Abbott, R., Abbott, T. D., Abraham, S., et al. 2021,  
 182 SoftwareX, 13, 100658, doi: [10.1016/j.softx.2021.100658](https://doi.org/10.1016/j.softx.2021.100658)  
 183 Ashton, G., Hübner, M., Lasky, P. D., et al. 2019, ApJS,  
 184 241, 27, doi: [10.3847/1538-4365/ab06fc](https://doi.org/10.3847/1538-4365/ab06fc)  
 185 Hogg, D. W. 1999, arXiv e-prints, astro.  
 186 <https://arxiv.org/abs/astro-ph/9905116>  
 187 Talbot, C., Smith, R., Thrane, E., & Poole, G. B. 2019,  
 188 PhRvD, 100, 043030, doi: [10.1103/PhysRevD.100.043030](https://doi.org/10.1103/PhysRevD.100.043030)  
 189 Talbot, C., & Thrane, E. 2018, ApJ, 856, 173,  
 190 doi: [10.3847/1538-4357/aab34c](https://doi.org/10.3847/1538-4357/aab34c)  
 191 The LIGO Scientific Collaboration, the Virgo  
 192 Collaboration, the KAGRA Collaboration, et al. 2021,  
 193 arXiv e-prints, arXiv:2111.03634.  
 194 <https://arxiv.org/abs/2111.03634>  
 195 Veitch, J., Raymond, V., Farr, B., et al. 2015, PhRvD, 91,  
 196 042003, doi: [10.1103/PhysRevD.91.042003](https://doi.org/10.1103/PhysRevD.91.042003)